Journal of Advanced Research 39 (2022) 147–156

Contents lists available at ScienceDirect

Journal of Advanced Research

journal homepage: www.elsevier.com/locate/jare

Original Article

Virucidal and biodegradable specialty cellulose nonwovens as personal protective equipment against COVID-19 pandemic

Chao Deng [a], Farzad Seidi [a,*], Qiang Yong [a,*], Xiangyu Jin [c], Chengcheng Li [a], Ling Zheng [a], Zhenghong Yuan [d], Huining Xiao [b,*]

[a] International Innovation Center for Forest Chemicals and Materials and Jiangsu Co-Innovation Center for Efficient Processing and Utilization of Forest Resources, Nanjing Forestry University, Nanjing 210037, China
[b] Department of Chemical Engineering, University of New Brunswick, Fredericton, NB E3B 5A3, Canada
[c] Engineering Research Center of Technical Textiles, Ministry of Education, College of Textiles, Donghua University, Shanghai 201620, China
[d] Key Laboratory of Medical Molecular Virology (MOE/NHC/CAMS), Department of Medical Microbiology and Parasitology, School of Basic Medical Sciences, Shanghai Medical College, Fudan University, Shanghai 200032, China

HIGHLIGHTS

- Enable to instantly inactivate SARS-CoV-2 (>99.14%) and HCoV-229E (>98.83%).
- Excellent growth inhibition (>99.51%) towards both *E. coli* and *S. aureus*.
- Address the environmental concerns raised by non-biodegradable face masks.
- Development of safe, comfortable, and biodegradable textiles for PPE.
- A facile and scalable method to produce biocidal textiles for various applications.

GRAPHICAL ABSTRACT

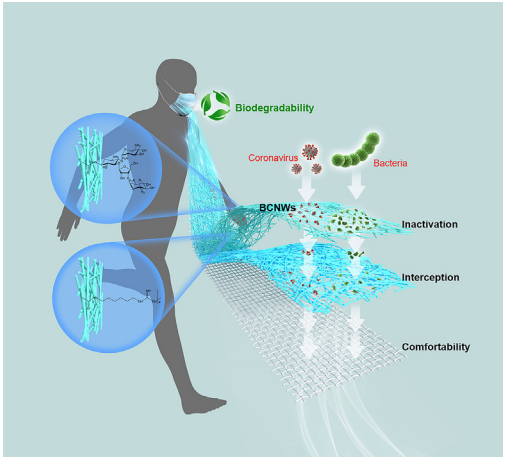

ARTICLE INFO

Article history:
Received 2 August 2021
Revised 29 September 2021
Accepted 3 November 2021
Available online 09 November 2021

Keywords:
Cellulose
Nonwoven
Antiviral
Antibacterial
Face mask
COVID-19

ABSTRACT

Introduction: Face masks are regarded as effective Personal Protective Equipment (PPE) during the COVID-19 pandemic. However, the dominant polypropylene (PP)-based masks are devoid of antiviral/antibacterial activities and create enormous environmental burdens after disposal.
Objectives: Here we report a facile and potentially scalable method to fabricate biodegradable, breathable, and biocidal cellulose nonwovens (BCNWs) to address both environmental and hygienic problems of commercially available face masks.
Methods: TEMPO-oxidized cellulose nonwovens are rendered antiviral/antibacterial via covalent bonding with disinfecting polyhexamethylene guanidine or neomycin sulfate through carbodiimide coupling chemistry.
Results: The obtained results showed that the BCNWs have virucidal rate of >99.14%, bactericidal efficiency of >99.51%, no leaching-out effect, and excellent air permeability of >1111.5 mm s^{-1}. More importantly, the as-prepared BCNWs can inactivate SARS-CoV-2 instantly.

Peer review under responsibility of Cairo University.
* Corresponding authors.
E-mail addresses: f_seidi@njfu.edu.cn (F. Seidi), swhx@njfu.com.cn (Q. Yong), hxiao@unb.ca (H. Xiao).

https://doi.org/10.1016/j.jare.2021.11.002
2090-1232/

Conclusions: This strategy provides a new platform for the green fabrication of multifunctional cellulose nonwovens as scalable bio-protective layers with superior performance for various PPE in fighting COVID-19 or future pandemics. Additionally, replacing the non-biodegradable non-antimicrobial PP-based masks with the cellulose-based masks can reduce the plastic wastes and lower the greenhouse gas production from the incineration of disposed masks.

Introduction

The devastating and highly contagious coronavirus disease (COVID-19) pandemic has led to infections on hundreds of millions of people, resulting in inestimable and irretrievable socioeconomic losses [1]. To alleviate the pandemic crisis, using the personal protective equipment (PPE) such as face masks is regarded as an important strategy to constrain and mitigate the transmission of concealed severe acute respiratory syndrome coronavirus 2 (SARS-CoV-2) [2]. However, the current polypropylene (PP)-based face masks without biocidal activity cannot eliminate the risk of infection entirely due to the longtime life of microorganisms on the mask surface [3]. Additionally, the performance and filtration efficiency of PP-based masks greatly depends on the electrostatic charges of masks which are disappeared generally after 8 h of utlizing the mask and make it necessary to be replaced by a new one [4]. The current consumption of face masks is over 200 million pieces per day [5] which results in an enormous burden of non-biodegradable PP plastic pollution. Practically, the increased plastic pollution from COVID-19 pandemic reminds scientists the importance to replace non-biodegradable goods with the biodegradable ones mostly based on natural polymers such as chitin, cellulose, starch, and lignin [6]. Simple replacing the PP-based mask by various types of cloth masks can address the issue related to the biodegradability pollution. However, the filtration efficiency for cloth masks was reported to be only ~80% for aerosols <300 nm and ~90% for aerosols >300 nm [7]. More advanced face masks such as N95, KN95, FFPs, and so on are generally able to exclude >95% of airborne particles [8,9]. However, all these masks still are suffering from non-biocidal activity and moreover, the disposed masks can act as a source of virus for secondary transmission of diseases. Therefore, the fabrication of virucidal/bactericidal face masks is of great significance for guaranteeing the safety of the disposed masks.

Extensive research has been conducted to fabricate antibacterial/antiviral materials relevant to face masks [10–13], such as incorporating the metal nanoparticles [14], essential oils [15], inorganic salts [16], and quaternary ammonium compounds [17] into face masks. However, leaching-out of nanoparticles and poor adhesion of water-soluble disinfectants with the mask become significant issues in consideration of the safety and long-term effectiveness of the masks [18]. Photo/electrothermal or photosensitizers-induced antimicrobial face masks [19,20] have shown effective and high inactivation activity, long-term durability, and broad-spectrum antibacterial property. However, most of these functional face masks require external triggers such as light, pressure and voltage, which practically puts limitations on applications. Polyurethane-coated face mask [21] has good breathability, durability, reusability, and can inhibit the adsorption of viruses and bacteria. However, the highly infectious pathogen can survive on these face masks which are lack of self-inactivation function. More importantly, the above functional modifications are based on non-biodegradable polypropylene (PP) fabrics that still raises the concerns on huge consumption of petroleum resources and significant environmental pollution. In fact, electrospinning nanofiber nonwoven fabrics have been developed using polylactic acid/chitosan [22], gluten [23], silk fibroin [24], and licorice extract [25] as biodegradable layer in face masks, but the major problem associated with the electrospinning nonwoven fabrics is their somehow decrease breathability [26]. More importantly, none of those materials are endowed with antiviral activity. To solve these problems, developing biobased or compostable nonwoven fabrics with virucidal properties along with antibacterial activity represent a very promising solution for creating biodegradable and multi-functional face masks. Prior to customizable-preparing such innovative nonwoven fabrics, two challenges must be addressed: 1) covalently grafting the virucidal or disinfecting agents as a guarantee of sustainability and long-term effectiveness of face masks; and 2) identifying biobased nonwoven fabric with desirable porous structures for excellent biodegradability and breathability.

Here, we develop a facile methodology to create biodegradable, breathable, and virucidal cellulose nonwovens (BCNWs). Cellulose is the most abundant natural resources on Earth, and bears a number of active hydroxyl groups which can be easily modified by antimicrobial agents [27]. We selected guanidine-based polymer, especially polyhexamethylene guanidine (PHG) that has strong antibacterial and antiviral properties [28,29], and neomycin sulfate (NEO), a kind of water-soluble aminoglycoside antibiotic with high antimicrobial activity [30] as virucidal agents in the current work. Both PHG and NEO can be readily covalent-grafted on the TEMPO-oxidized cellulose nonwovens (TOCNWs) via the amide formation. Despite that PHG and NEO are well known for their activities against a broad spectrum of bacteria and certain types of viruses [31,32], it is still unknown whether the grafting of those two agents on TOCNWs in such a manner can create sufficiently high antiviral activity against coronavirus, SARS-CoV-2 in particular. Therefore, this work presents the first attempt on grafting the tailor-selected functional polymer or agent on TEMPO-oxidized cellulose nonwovens to endow the nonwovens with superior virucidal performance. The prepared nonwovens in this work exhibited the integrated properties of biodegradability, high virucidal and bactericidal efficacy, excellent breathability, and long-term effectiveness. Therefore, the incorporation of BCNWs as a green bio-protective layer into the face masks enables the superior protection against SARS-CoV-2 and bacteria, whereas the application can be extended to other types of PPE materials like body protection suit/gown and textiles for hospital uses, thus magnifying the benefits further.

Materials and methods

Materials and chemicals

Pristine cellulose nonwovens (CNWs) with excellent breathability and biodegradability, were prepared by wet-laid formation followed by hydroentanglement consolidation as described previously [33,34], in which 20 wt% bleached softwood pulp (fiber length of 2.4–2.6 mm, width of 34.7 ± 9.2 μm, and thickness of 5.0 ± 1.8 μm) and 80 wt% Lyocell fibers (fiber length of 12 mm, diameter of 11.9 ± 1.1 μm) were homogeneously mixed in a fiber mixing chest. The mixed fiber slurry was pumped to a hydroformer

to form the wet-laid fiber web which was consolidated by water jets to obtain the CNWs. The pore size distribution of the as-prepared CNWs is presented in Fig. S1.

2,2,6,6-Tetramethylpiperidine 1-oxyl (TEMPO, 98%), sodium bromide (NaBr, 99%), sodium hypochlorite solution (NaClO, 6–14%), 1-ethyl-3-(3-dimethylaminopropyl)-carbodiimide (EDC, 98%), N-Hydroxysuccinimide (NHS, 98%) and neomycin sulfate (NEO, USP grade) were purchased from Aladdin Biochemical Technology Co., LTD. Polyhexamethylene guanidine (PHG) was self-synthesized via the condensation polymerization described in our previous work [35]. Sodium hydroxide and hydrochloric acid were purchased from Nanjing Chemical Co., LTD and ethanol was purchased from Wuxi Yasheng Chemical Co., LTD.

Fabrication of antibacterial and antiviral CNWs

CNWs were firstly cut into a rectangular shape of size 14 × 16 cm^2 with a thickness of approximately 500 μm (see Table S1 for details), then immersed in the reacting solution consisting of 21.6 mg TEMPO, 270 mg NaBr, 140 mL of deionized (DI) water, and NaClO at a pre-designed amount to keep pH of the solution at 10; and the oxidation reaction proceeded for approximately 4 h. Afterwards, the TEMPO-oxidized CNWs (TOCNWs) were washed with DI water for three times and then ethanol for one time and dried at ambient temperature. After drying, the TOCNWs were added in 108 mL of EDC (20 mg L^{-1}) and NHS (20 mg L^{-1}) reacting solution for 30 min. Subsequently, PHG and NEO aqueous solutions at different concentrations with the pH of 7.5–8.0 were added in the former reaction system for 24 h at ambient temperature. Finally, the as-prepared TOCNWs-PHG and TOCNWs-NEO were washed with DI water (three times) and then ethanol (one time) and dried at ambient temperature.

Antibacterial assays using E. coli and S. aureus

The colony method was adopted to quantitatively evaluate the inhibition efficiency of cell growth. Firstly, the bacterial strains (*E. coli* and *S. aureus*) were incubated overnight in Luria-Bertani (LB) broth medium with shaking at 200 rpm at 37 °C. Then, the bacterial suspension was diluted with LB broth to a concentration of 5 × 10^6 colony-forming units (CFU)/mL. After that, 0.01 g TOCNWs-PHG (TOCNWs-NEO) sample was added in 5 mL of diluted bacterial suspension in the vial, and subsequently cultured in a shaking incubator (200 rpm) at 37 °C for 10 min and 60 min, respectively. Finally, the resulting bacterial suspensions (100 μL) were spread on gelatinous LB agar plates respectively, culturing at 37 °C for 24 h. The number of survival colonies was counted, and the growth inhibition rate (GIR) was defined by the formula: GIR=(A-B)/A × 100%, in which the A and B are the number of the bacterial colonies counted from the control and TOCNWs-PHG (TOCNWs-NEO) samples, respectively. The assays were repeated three times for each bacterium.

Antiviral assays using HCoV-229E virus

The HCoV-229E virus was propagated on the Madin-Darby Canine Kidney (MDCK) and incubated in the maintenance medium (800 mL of grade 3 water, 60 mg kanamycin sulfate and 9.53 g agle's minimum essential medium), Trypsin and PBS solution at 34 °C. The prepared virus suspension (0.2 mL) was spotted on the surface of modified CNWs or control samples with a size of 20 × 20 mm^2 in the vial containers, and then, the samples in the vials were incubated at 25 °C for 60 min. Afterwards, 20 mL of Soybean Casein Digest Lecithin Polysorbate (SCDLP) medium were added in the vials and thereafter, the vials were vortexed for 5 s and 5 times to wash out the virus from the samples. After serial dilution, 0.1 mL of virus suspension was mixed with MDCK cells seeded previously at a density of 10^4 cells per well, followed by incubation for 1 h at 34 °C with 5% CO_2. After that, 0.2 mL of the maintenance medium was added, and the plates were incubated at 34 °C with 5% CO_2. After 7 days, each cell in the wells was observed using an inverted optical microscope to monitor the cytopathy of the cell. $TCID_{50}$ was calculated according to the Behrens and Karber method.

Antiviral assays using SARS-CoV-2 virus

In a typical titer assay, the VeroE6 cells were seeded in 96-well plates one day prior to the experiment and used to propagate the SARS-CoV-2 SH01 strain (GenBank accession no. MT121215). A total of 100 μL (20 μL each drop) of the virus suspension was spotted on the surface of BCNWs samples in a size of 20 × 20 mm^2, and then, the BCNWs samples were exposed for a certain time at 25 °C. The BCNWs samples with the virus were vortexed for 5 s and stirred for 5 times in a tube containing 10 mL of EBSS at each time point. After serial dilution by mixing the virus suspension and maintenance medium (1:9), the virus dilutions (100 μL) were added in each well and cultured for 1 h at 37 °C with 5% CO_2. Then, each well was added 100 μL of methyl cellulose and incubated for 48 h at 37 °C with 5% CO_2. After that, 200 μL of 4% paraformaldehyde were added in each well for 30 min. Subsequently, the solutions in the plate were transferred to 0.2% saponin solution for stanning. Cells were stained with rabbit against SARS-CoV-2 N protein polyclonal antibody overnight at 4 °C, and then incubated with the secondary goat anti-rabbit horseradish peroxidase (HRP)-conjugated antibody for 1 h at room temperature. TrueBlue substrate (Sera Care #5510–0030) was added to develop the focus-forming unit. The inverted microscopy was used to count the plaques which were reported as PFU mL^{-1}. All data were standardized as 1 × 10^5 PFU initial load and plotted PFU (plaque-forming unit).

Inhibition zone assay

The assay for visualizing the inhibition zone was conducted to evaluate the leaching-out effect of the disinfectants incorporated into the BCNWs against both *E. coli* and *S. aureus* strains. Prior to the assay, both *E. coli* and *S. aureus* strains were incubated in Luria-Bertani (LB) broth medium overnight with shaking at 200 rpm at 37 °C. Then, 100 μL of bacterial suspensions (5 × 10^6 CFU/mL) were uniformly coated on the LB agar plate. Afterwards, the BCNWs samples in a diameter of 6 mm were placed in the bacterial inoculated agar plate, and then incubated at 37 °C for 24 h. The size of the inhibition zone was finally measured to assess the leaching-out effect of the samples.

Cell viability assays

Cytotoxicity of antibacterial and antiviral CNWs was assessed using a 3-(4,5-dimethylthiazol-2-yl)-2,5-diphenyl-2H-tetrazolium bromide (MTT) assay on NIH3T3 cells (from mouse embryonic fibroblasts) which were cultured in cell growth media (87% Dulbecco's Modified Eagle Medium (DMEM), 10% fetal bovine serum (FBS), 1% sodium pyruvate, 1% glutamine, and 1% nonessential amino acids). Samples were pretreated by UV-sterilization at each side for 30 min, and then placed in a 48-well plate. 100 μL of growth medium was used as control. Subsequently, the cultured NIH3T3 cells were seeded on the CNWs samples with an initial density of 1 × 10^4 cells per well and incubated at 37 °C in the 5% CO_2 incubator. After 24 h, CNWs samples and growth medium were removed, and each well was washed with PBS for three times. Afterwards, 200 μL of growth medium containing MTT (0.5 mg mL^{-1}) was added in each well and incubated at 37 °C in

the 5% CO_2 incubator for 4 h. After the incubation, 200 μL of dimethyl sulfoxide (DMSO) was added, and the mixed solutions were gently shaken for 10 min. The absorbance change was observed at 570 nm to determine the cell viability.

Biodegradation test

Five types of nonwovens were prepared for biodegradation tests, including TOCNWs-PHG, TOCNWs-NEO, CNWs, blue polypropylene spunbond nonwovens (PP SBNWs-1), and white polypropylene spunbond nonwovens (PP SBNWs-2). Test samples with size of 2.5 × 2 cm^2 were buried in nutrient soil and watered regularly. To observe the morphological change of samples for various periods (after 10, 20, 30, and 40 days), samples were dug out of the soil and recorded.

Characterization

SEM images were examined by a Hitachi Regulus 8100 SEM working at an acceleration voltage of 5 kV. Fourier-transform infrared (FTIR) spectra were collected with a VERTEX80v spectrometer (Bruker Optik GmbH, Germany). X-ray photoelectron spectrometer (XPS) spectra were recorded on an AXIS UltraDLD spectrometer (Kratos, UK). The element content data of samples were collected with an elemental analyzer (2400 Ⅱ, Perkin Elmer, USA). A T200-Auto 3 Plus contact angle analyzer (BiolinScientific, Germany) was used to conduct the water contact angle test, in which a drop of distilled water (4 μL) from a micro syringe was automatically dispensed on the surface of sample. A digital air permeability tester (YG461E, Wenzhou Fangyuan Instrument Co., Ltd, China) (Fig. S2) was used to evaluate the air permeability. An Automated Filter Tester 8130 (TSI Inc., USA) (Fig. S3) was used to measure the filtration efficiency and pressure drop with a flow rate of 85 L min^{-1}, and sodium chloride (NaCl) monodisperse aerosols with a mass median diameter of 0.26 μm were used as the model particles.

Results and discussion

Synthesis of antibacterial and antiviral CNWs

Fig. 1a presents an overview of the synthesis of TOCNWs-PHG/NEO via TEMPO oxidation followed by disinfectant grafting. The pristine cellulose nonwovens (CNWs) were pretreated by TEMPO/NaBr/NaClO oxidation to increase the number of the reactive sites (carboxyl groups) on the surface of CNWs. Subsequently, grafting reactions were conducted by immersing the TEMPO-oxidized CNWs (TOCNWs) in PHG or NEO solutions with various concentrations. The amide formation between the carboxyl groups on the TOCNWs and primary amino groups of PHG or NEO, i.e., carboxyl-to-amine crosslinking, was promoted by 1-ethyl-3-(3-dimethylaminopropyl)-carbodiimide (EDC) and N-hydroxysuccinimide (NHS)-mediated covalent coupling reaction (Fig. S4). Thereafter, the resultant modified TOCNWs were washed with deionized water (DI) and ethanol to remove any residual agents. The TOCNWs modified by PHG and NEO are abbreviated as TOCNWs-PHG and TOCNWs-NEO, respectively. The representative optical images of the relevant samples are shown in Fig. 1b and Fig. S5, which indicated no obvious changes of morphology of CNWs after modification. The as-prepared nonwoven can act as a multi-functional outer layer of the mask to effectively inactivate the bacteria and viruses (including coronavirus) upon the exposure or contact. Due to well-designed structure of CNWs and low dosage of disinfectants, the excellent breathability and biodegradability of the nonwoven with superior virucidal activity are maintained (Fig. 1c).

Characterization of BCNWs

To demonstrate the successful covalent conjugation between the guanidine-based polymer or NEO and CNWs, FTIR spectra corresponding to each step of the reactions are presented in Fig. S6. A new absorption peak at 1608 cm^{-1} in the spectrum of TOCNWs was assigned to the stretching band of the sodium carboxylate groups (-COONa), which confirmed the successful TEMPO oxidization on the surface hydroxyl groups of CNWs. The successful grafting of the PHG on TOCNWs was confirmed by the peak at 1636 cm^{-1}, which is ascribed to C=N stretching vibration and suggested the existence of PHG in the sample. No specific strong peaks can be detected for the NEO grafting from FTIR, which, however, has been confirmed from the XPS results shown below.

The grafting of different chemicals on CNWs via covalent bonding was further identified from the X-ray photoelectron spectroscopy (XPS) spectra (Fig. 2a-2f). Apparently, the Na 1s peak appeared in the TOCNWs (Fig. 2a), indicating the presence of the sodium carboxylate groups when compared with the XPS wide scan spectrum of CNWs. Meanwhile, comparing the C 1s core-level spectra of TOCNWs (Fig. 2c) with that of CNWs (Fig. 2b), the new peak with binding energy of 287.7 eV corresponding to the O-C=O occurred, suggesting the formation of carboxyl groups after TEMPO oxidization. The C 1s core-level spectra of TOCNWs-PHG (Fig. 2d) displayed several peaks with binding energies of 284.6, 286.3, 288.7, 285.0, 287.6 and 288.4 eV, which were assigned to the C-C, C-O, C=O/O-C-O, C-N, O-C=O and C=N groups, respectively. Noting that a new peak at 288.4 eV (C=N) demonstrated the successful attachment of PHG to TOCNWs. The C 1s core-level spectra of TOCNWs-NEO were curved and fitted to 284.6 eV for C-C species, 286.6 eV for C-O species, 288.7 eV for C=O/O-C-O species, 285.0 eV for C-N species, and 287.7 eV for O-C=O species, respectively. Among them, the success of grafting NEO onto the surface of TOCNWs was especially confirmed by the new C-N peak at 285.0 eV (Fig. 2e). Moreover, the successful conjugation of PHG onto the TOCNWs was confirmed by the new peak N=C at 400.4 eV (Fig. 2f). Overall, the results from XPS clearly demonstrated the success in the preparation of TOCNWs-PHG and TOCNWs-NEO via covalent grafting.

Nitrogen content obtained by elemental analysis was used to estimate the quantity of PHG and NEO in the modified TOCNWs. According to the results (Table S2), in the absence of NHS around 96.1 mg g^{-1} PHG moieties incorporated in TOCNWs while the C_{PHG} for TOCNWs-NHS-PHG was slightly higher, i.e., 122.6 mg g^{-1}. Indeed, NHS improved the activation of the carboxyl groups of amino acids in the reaction process and therefore, higher grafting contents could be obtained. The C_{NEO} of TOCNWs-NEO (155.7 mg g^{-1}) was much higher than that of TOCNWs-PHG. This result can be attributed to more amino groups on NEO molecule chain; and it also has less steric effect than polymeric PHG, thus resulting in higher grafting amount.

The representative field-emission scanning electron microscopy (FE-SEM) images of the relevant samples at different reacting steps presented in Fig. 2g revealed the randomly oriented three-dimensional nonwoven morphology with small holes on the material surface. It should be noted that no obvious morphological changes of the sample surface were observed after the TEMPO oxidization and polymer grafting, which in turn guarantees the appropriate air permeability of CNWs even after the modification. Despite the high concentration of TEMPO/NaClO reagents can severely degrade the cellulose nanofibrils [36], the more persistent microfiber structure of CNWs treated with low concentration of TEMPO/NaClO reagents in the current work was observed. Fig. 2h demonstrates the feasible applications of antibacterial and antiviral CNWs in respirator and medical face mask. The TOCNWs-PHG are as flexible as traditional nonwovens used in mask filter media

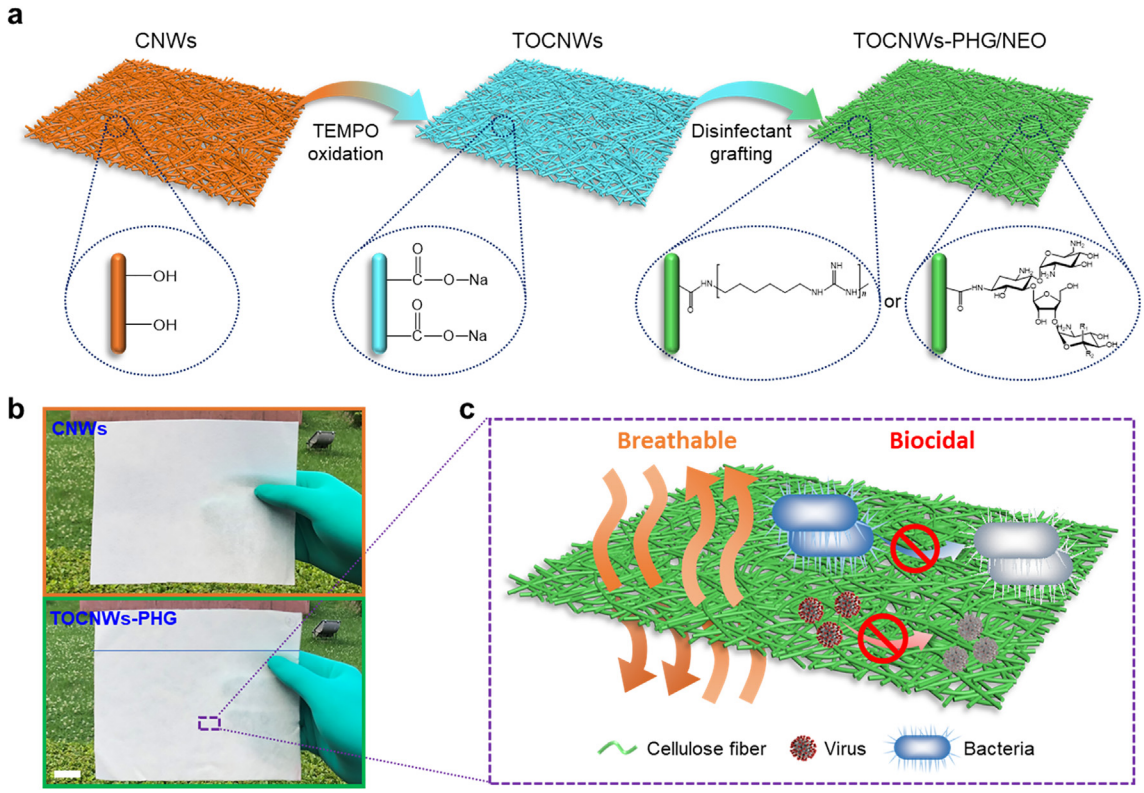

Fig. 1. Fabrication of antibacterial and antiviral CNWs. (a) Schematic illustration of the synthesis of biocidal TOCNWs-PHG/NEO. (b) Optical images of CNWs and TOCNWs-PHG (scale bar: 2 cm). (c) Schematic demonstration of breathability and biocidal ability of TOCNWs-PHG/NEO.

and can be readily folded, pleated, rolled-up, and recovered (Fig. S7), so do the TOCNWs-NEO samples (Fig. S8). It should be noted that the water contact angle (WCA) of CNWs was changed slightly after the grafting of the antimicrobial agents (Fig. S9). The initial WCA of TOCNWs-PHG (98.6°) increased moderately compared to that of pristine CNWs (74.1°), which might be ascribed to the less hydrophilic long chain structure of PHG. However, similar to CNWs, the WCAs of both TOCNWs-PHG and TOCNWs-NEO exhibited rapid reduction to 0° after 0.25 s (Fig. S9), due to the bulky three-dimensional and porous structures (Fig. 2g).

Antibacterial and antiviral properties of BCNWs

Prior to assessing virucidal performance, the killing efficiencies of the TOCNWs-PHG and TOCNWs-NEO was evaluated first. We challenged the BCNWs as well as pristine CNWs with two typical pathogenic bacteria, Gram-negative *Escherichia coli* (*E. coli*) and Gram-positive *Staphylococcus aureus* (*S. aureus*). For the antibacterial assay, the samples with a weight of 0.01 g were mixed with 5 mL of bacterial suspension (5×10^6 CFU/mL), and the bacterial proliferation was assessed using a colony count method. The pristine CNWs exhibited poor killing efficiencies reaching 26.16% ± 1.30% (*E. coli*) and 28.11% ±1.95% (*S. aureus*) at 60-min contact time (Fig. S10), which might be induced by the sulfate remained in the fabrication of pulp fiber. As for TOCNWs-PHG, the time-dependent antibacterial effect is shown in Fig. 3a. Clearly, the TOCNWs-PHG showed effective inactivation of bacteria, achieving the killing efficiencies of >99% of *E. coli* and *S. aureus* in 10- and 30-min contact time, respectively. The results suggested the stronger inhibitory effect of the TOCNWs-PHG on the growth of *E. coli* strains than that of *S. aureus* strains. As for TOCNWs-NEO, the killing efficiencies of >99% of *E. coli* and *S. aureus* were obtained in 30- and 10-min contact time, respectively, which appears to be opposite to the inactivation activities of TOCNWs-PHG against *E. coli* and *S. aureus* (Fig. 3b). Therefore, it is speculated that NEO polymer has better disinfecting capability against *S. aureus* compared to *E. coli* within short time. This might be due to the fact that the cell membrane constituent of *S. aureus* has an outer peptidoglycan layer that can be inactivated and destroyed easily by NEO, thus allowing NEO to penetrate inside the cell to bound with the DNA and to deactivate the organisms. In contrast, the outer phospholipid membrane of *E. coli* is relatively easy to be deteriorated by PHG. Moreover, killing efficiency of the BCNWs with various disinfectant dosages were investigated. Evaluation of the parent biocidal agents showed that both PHG and NEO exhibited excellent killing efficiencies (>99%) against E. coli and S. aureus after 15-min contact time even under the lowest starting concentration (0.1 mg mL^{-1}) (Fig. S11). As shown in Fig. 3c, the killing efficiencies of TOCNWs-PHG against the *E. coli* and *S. aureus* increased with the increasing concentration of disinfectants after 15-min contact time. However, the TOCNWs-PHG showed better inactivation activities on *E. coli* compared with *S. aureus*, which are consistent with the results displayed in Fig. 3a. Meanwhile, the increasing killing efficiencies of TOCNWs-NEO against the *E. coli* and *S. aureus* were also observed when the concentration of disinfectants was increased (Fig. 3d), while TOCNWs-NEO was more effective against the *S. aureus* than *E. coli*. Moreover, the killing efficiency of the TOCNWs-NEO against the *E. coli* was only 86.28% ± 1.42% even the concentration of NEO reaching 100 mg mL^{-1}, indicating the time-dependent inactivated effect of the TOCNWs-NEO against the *E. coli*. To demonstrate the durability of BCNWs, the samples were placed in water under constant stirring for 30 min at room temperature to simulate the daily washing of face masks (Fig. S12a). After 15-min contact with bacteria (Fig. S12b), the washed BCNWs still

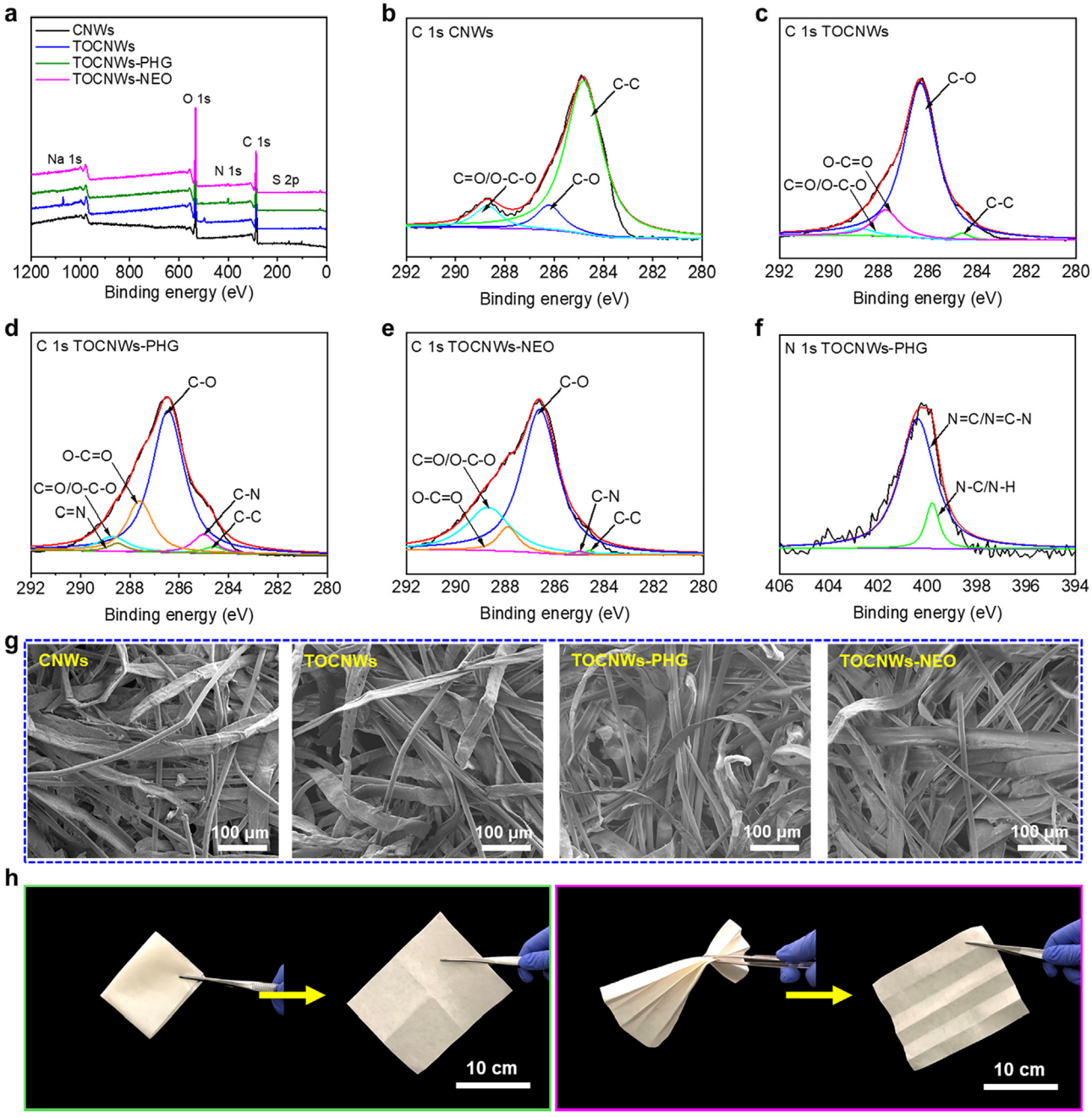

Fig. 2. Characterizations of BCNWs. a) Wide scan XPS spectra. b-e) C 1s core-level spectra of CNWs, TOCNWs, TOCNWs-PHG, and TOCNWs-NEO. f) N 1s core-level spectra of TOCNWs-PHG. g) SEM images of the microscopic structures of CNWs at different grafting steps. h) Optical images of virucidal TOCNWs-PHG that can be folded, pleated, and recovered.

kept high killing efficiencies that are comparable with those of the unwashed BCNWs (Fig. 3c and 3d, 100 mg mL^{-1}) against S. aureus in particular.

Antiviral function or behavior is the key focus of the current work, and of the most importance for us to judge whether the bioprotective PPE materials can effectively inactivate viruses, especially for SARS-CoV-2, thereby benefiting the fight against the COVID-19 pandemic nowadays. To evaluate the antiviral performance of the BCNWs, we tested the TOCNWs-PHG and TOCNWs-NEO against both HCoV-229E (Human coronavirus) and SARS-CoV-2 viruses and assessed the cytopathic effect using a Titer assay. HCoV-229E, a type of coronavirus, is an enveloped single-stranded RNA virus, which has been shown to have less virulent capacity [37]. Therefore, HCoV-229E is an appropriate surrogate on several BCNWs samples prior to the SARS-CoV-2 inactivation tests. As shown in Fig. 3e, nearly no contact inactivation was observed on the unmodified CNWs ($10^{6.47}$ $TCID_{50}$/mL) compared to that of control virus suspension ($10^{6.66}$ $TCID_{50}$/mL), and the harvested phages could grow and proliferate freely in the culture medium. In contrast, both TOCNWs-PHG and TOCNWs-NEO showed effective inactivation of HCoV-229E phage, achieving titers of $10^{4.72}$ and $10^{4.55}$ $TCID_{50}$/mL, respectively, after 60-min contact exposure. In comparison, the TOCNWs-NHS-PHG had a lower titer value ($10^{4.09}$ $TCID_{50}$/mL) compared to that of TOCNWs-PHG, which could be explained by the improved reactivity due to the addition of NHS, thus resulting in higher

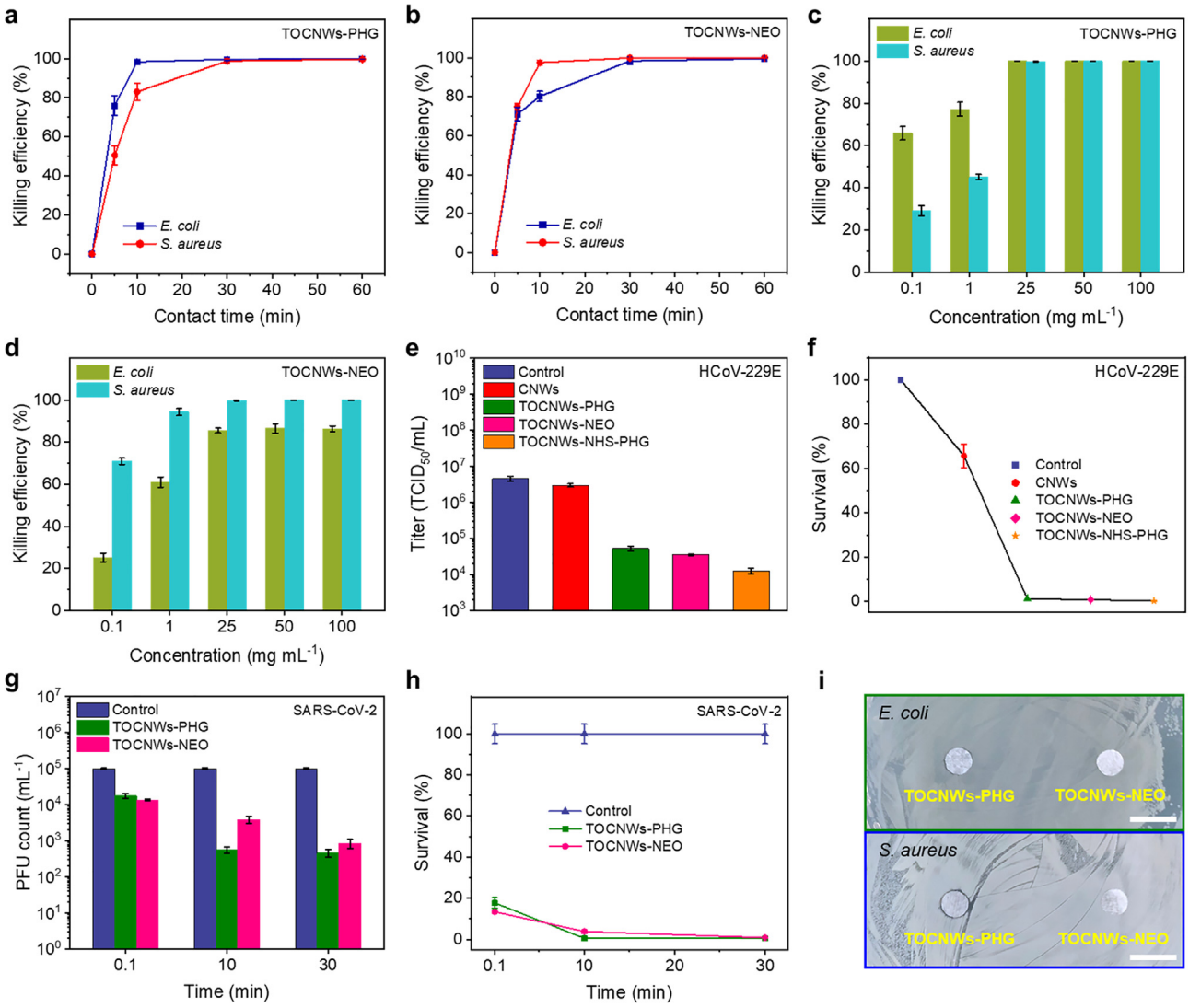

Fig. 3. Antibacterial and antiviral properties of BCNWs. a) Killing efficiency of TOCNWs-PHG against *E. coli* and *S. aureus*. b) Killing efficiency of TOCNWs-NEO against *E. coli* and *S. aureus*. c) Killing efficiency of TOCNWs-PHG with various dosages. d) Killing efficiency of TOCNWs-NEO with various dosages. e) Infectivity of the HCoV-229E virus on different BCNWs. f) Survival of the HCoV-229E virus on different BCNWs. g) Infectivity of the SARS-CoV-2 virus on different BCNWs. h) Survival of the SARS-CoV-229E virus on different BCNWs. i) Inhibition zone images of BCNWs against *E. coli* and *S. aureus* (scale bar: 10 mm).

grafting amount of guanidine-based polymer on the surface of CNWs. To express the antiviral performance of virucidal CNWs more intuitively, Fig. 3f presents the results compiled in the form of HCoV-229E survival which is defined as the ratio of a titer at a given exposure time normalized relative to that of the control virus suspension multiplied by 100% (Table S3). As shown in Fig. 3f, the survivals of HCoV-229E phages were 1.17% ± 0.15%, 0.78% ± 0.13%, and 0.28% ± 0.07% for the TOCNWs-PHG, TOCNWs-NEO, and TOCNWs-NHS-PHG, respectively. These positive findings from the HCoV-229E antiviral assay proved that the cellulose-based nonwovens grafted with the reactive chains containing PHG and NEO segments are highly virucidal to the coronavirus. More importantly, the excellent inactivation abilities of the BCNWs demonstrated by HCoV-229E antiviral assay literally encouraged us to proceed with identifying their inactivation activity against SARS-CoV-2, which is critical for the application of the antiviral masks or textiles in the current pandemic or even afterwards.

As shown in Fig. 3g, both TOCNWs-PHG and TOCNWs-NEO exhibited rapid and effective inactivation of SARS-CoV-2 virus, achieving 0.75, 0.87 and 2.33, 2.07 log 10 reduction in PFU (plaque-forming units) after ~0.1- and 30-min contact time, respectively (Table S4), which highlighted the fast and highly virucidal activities. These positive results, especially after momentary contact (~0.1 min), demonstrated the effectiveness of the BCNWs in rapidly inactivating SARS-CoV-2 for the first time since such superior performance has never been reported previously for the cellulose-based nonwoven antiviral-modified in the manners developed in the current work. Noteworthily, TOCNWs-PHG showed better inactivation ability when compared to TOCNWs-NEO within 10- and 30-min contact time, indicating that PHG is advantageous to inactivate the SARS-CoV-2 within short contact time. Meanwhile, the survival of SARS-CoV-2 after contacting the BCNWs is displayed as a function of exposure time in Fig. 3h. As can be seen, the survivals of SARS-CoV-2 after instant contact (~0.1 min) with TOCNWs-PHG and TOCNWs-NEO were 17.75% ± 2.60% and 13.48% ± 0.61%, respectively, revealing the instant inactivating abilities. As the exposure time was prolonged to up to 30 min, the inactivation rates of TOCNWs-PHG and TOCNWs-NEO reached as high as 99.54 ± 0.11% and 99.14% ± 0.24%, respectively, confirming the superior virucidal characteristics of the modified

BCNWs. In addition, compared with antiviral activities towards HCoV-229E aforementioned, the modified BCNWs exhibited even higher effectiveness in inactivating SARS-CoV-2, thus further validating the suitability of such-modified nonwoven as promising PPE to provide outstanding bio-protection against SARS-CoV-2, which is of great significance to the current COVID-19 pandemic. To further verify the leaching-out effect of disinfectants incorporated into the BCNWs, the inhibition zone assay [31,38] was performed. As shown in Fig. 3i, both TOCNWs-PHG and TOCNWs-NEO displayed no inhibition zone against *E. coli* and *S. aureus*, suggesting that the covalent grafting method can eliminate any the leaching-out or release of the virucidal agents from BCNWs substrates. Therefore, the safety of as-prepared BCNWs was further proved, allowing them to be promising materials incorporated in face masks or other types of PPE without inducing safety concerns.

The as-prepared BCNWs exhibited highly instant virucidal (>99.14%) and bactericidal (>99.51%) efficacy, which was ascribed to the biocidal function of PHG or NEO grafted on the surface of cellulose nonwovens. Up on exposure or contacting with the pathogen in aerosols or liquid form, the functionalized BCNWs networks captured or entrapped the viruses or bacteria firstly, and then inactivate the pathogens by the PHG or NEO grafted on the nonwoven surface. The lipid envelope of SARS-CoV-2 could be disorganized and damaged severely through the interaction of PHG segments with viral particles and therefore, leading to the leakage of the viral genome. Furthermore, considering the replication of virus infection requires the endosome with low pH [39], the viral infection might be inhibited by the endosomal pH that is neutralized by the unprotonated amine groups in guanidine-based polymers. The antiviral mechanism of neutralized endosomal pH might also be suitable for the amine groups presented in NEO. Moreover, NEO might be able to interact with the viral structural or bind to viral RNA specifically, thus resulting in the direct inactivation of SARS-CoV-2. It is also possible that NEO might directly inhibit the protein synthesis and viral translation, which reduces the viral RNA synthesis [40]. In particular, the antiviral results of NEO are consistent with reports that aminoglycosides inhibit replication of DNA and RNA viruses in several species [41]. Therefore, from a mechanistic point of view, the covalent grafting of PHG or NEO on the cellulose nonwovens promises the applications of the BCNWs in performance-enhanced face masks or other functional PPE.

Cytotoxicity, filtration property and biodegradability of BCNWs

Safety regulations for the use of PPE require disinfecting polymer or agent as well as relevant materials to have low cytotoxicity; and especially those bearing the minimal cytotoxicity are generally preferable to be accepted. To validate the surface cytotoxicity of the BCNWs created in this work, an in vitro MTT method and live/dead viability assays were adopted to analyze the cell viability. As shown in Fig. 4a, the MTT values of TOCNWs-PHG and TOCNWs-NEO were 84.32% ± 10.86% and 81.19% ± 9.19%, respectively, indicating good viability of NIH3T3 cells when contacting with the BCNWs. In comparison, the biocidal masks modified by AgNPs showed lower cell viability of ~30% even when the concentration of AgNPs is only 5 μg mL^{-1} [42]. Meanwhile, the results obtained from the visualization of the fluorescent images of live/dead assays (Fig. 4b-4d) showed that both TOCNWs-PHG and TOCNWs-NEO had little influence on the cell viability compared to the control sample, thus further demonstrating the desirable biosafety of the modified BCNWs as bioprotective PPE without causing any detriments of health even when directly contacting with the human body.

Considering the practical bio-protection applications associated with textile, face masks in particular, we further investigated the filtration property of the virucidal CNWs in conjunction with polypropylene meltblown nonwovens (PP MBNWs) which is typically used as a mid-layer in face masks to entrap fine aerogels and particles via electrostatic interaction. Meanwhile, the filtration property of a single PP MBNWs was also examined as a control to identify whether the virucidal CNWs layer has any impact on the filtration property of the entire filtering media. The evaluation of filtration performance was carried out using polydisperse sodium chloride (NaCl) particles as model particles for bacteria and viruses. The filtration efficiencies of single CNWs, TOCNWs-PHG, and TOCNWs-NEO were 8.23% ± 0.21%, 8.07% ± 0.15%, and 7.90% ± 0.20%, respectively (Fig. S13). After combining BCNWs with PP MBNWs, as shown in Fig. 4e, the filtration efficiencies of the TOCNWs-PHG and TOCNWs-NEO integrated with PP MBNWs were 99.40% ± 0.02% and 99.39% ± 0.02% (85 L min^{-1}), respectively, which were comparable with that of the single PP MBNWs (99.38% ± 0.04%), demonstrating no distinct negative effects when the functional virucidal CNWs are used as alternatives for other layers in face masks. Meanwhile, the pressure drops of the TOCNWs-PHG (119.03 ± 2.47 Pa) and TOCNWs-NEO (115.49 ± 3.4 4 Pa) integrated with PP MBNWs were increased compared to that of single PP MBNWs (93.22 ± 1.96 Pa) at the airflow of 85 L min^{-1}, which, however, was only a third of the standard pressure drop of N95 respirator (350 Pa at 85 L min^{-1}) [43]. To further prove the robust breathability of the virucidal CNWs, we measured the air permeability of the nonwoven using an air permeability tester with a pressure difference of 100 Pa. As shown in Fig. 4f, the air permeabilities of TOCNWs-PHG and TOCNWs-NEO were 1111.57 ± 59.41 mm s^{-1} and 1117.30 ± 55.32 mm s^{-1}, respectively, which is about 4 times as high as PP MBNWs (271.61 ± 7.20 mm s^{-1}). The high air permeability is desirable in wearing comfortability for face mask, which guarantees the superior performance of the face masks integrated with the virucidal BCNWs as a biodegradable substitute layer in filtering media. The promising filtration efficiencies were also confirmed by SEM observations. As can be seen from Fig. 4g, after filtration loading for 20 min, enormous sodium chloride particles were deposited on the fiber surface of PP MBNWs due to electrostatic attraction, which is crucial to the mask filtration efficiency. Meanwhile, the TOCNWs-PHG and TOCNWs-NEO can also capture or entrap some small particles on their fiber surface (Fig. 4h and 4i), implying that they may provide the barrier towards aerosols to some extent though rendering face masks virucidal is the key role.

To investigate the biodegradability of the BCNWs, TOCNWs-PHG and TOCNWs-NEO were buried in soil along with the pristine CNWs and two kinds of commercial outer layer of face masks (PP SBNWs-1 and PP SBNWs-2). As shown in Fig. S14, while petroleum-based PP SBNWs remained almost unchanged 40 days after burying, the CNWs and BCNWs were completely decomposed in around 30 and 40 days, respectively, demonstrating the excellent biodegradability of BCNWs in soil. Therefore, the incorporation of BCNWs in face masks can effectively alleviate the environmental burden caused by petroleum-based PPE in current and future pandemics.

Conclusion

A facile and effective strategy was developed for the scalable fabrication of biodegradable and antiviral/antibacterial materials through the covalent grafting of highly biocidal agents including polyhexamethylene guanidine (PHG) and neomycin sulfate (NEO) on cellulose nonwovens. The as-prepared biocidal cellulose nonwovens (BCNWs) can inactivate, within minutes, >99% of the

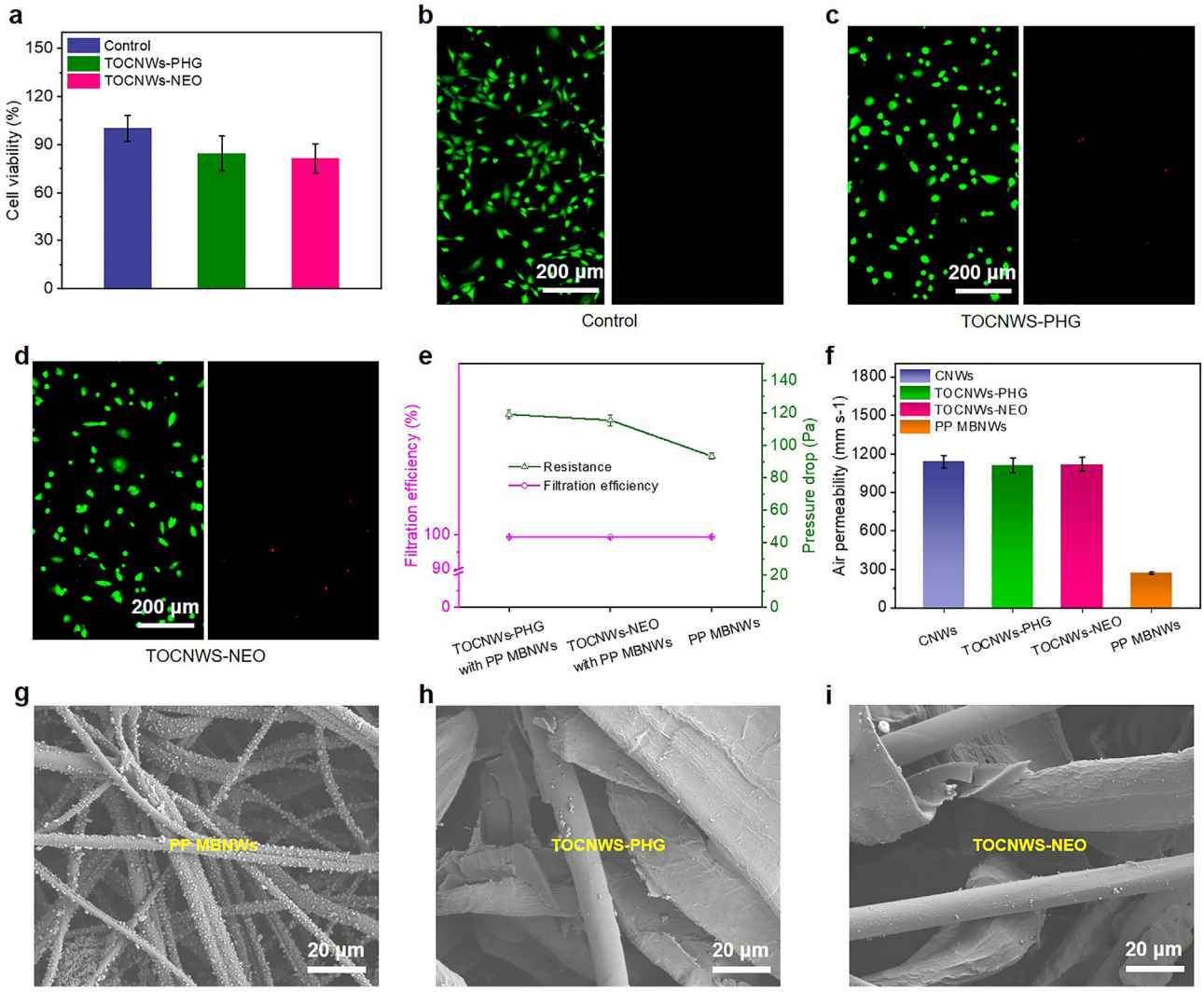

Fig. 4. Cytotoxicity and filtration properties of the BCNWs. a) The NIH3T3 cell viabilities after 24 h of contacting with different BCNWs. b-d) Live/dead images of control, TOCNWs-PHG, and TOCNWs-NEO. e) Filtration efficiency and pressure drop of BCNWs combined with PP MBNWs. f) Demonstration of good air permeability of BCNWs compared with PP MBNWs. g-i) SEM images of sodium chloride particles capture of PP MBNWs and BCNWs after the loading filtration test.

SARS-CoV-2, HCoV-229E viruses, and Gram-positive and Gram-negative bacteria. Additionally, biodegradability, low cytotoxicity, and excellent breathability of BCNWs enable them to be appropriate materials for face masks to achieve robust bio-protection without compromising the interception efficiency and negative impact on environment. Household textiles, industrial wipes, health-care materials, and air filters could also be made from BCNWs with tailored nonwoven structures whereas the strategy developed in this work for the efficiently grafting of virucidal segments remains applicable. The resultant biodegradable nonwovens are anticipated to satisfy the hygiene requirement of the public in the current COVID-19 pandemic and emerging infectious diseases in the future.

CRediT authorship contribution statement

Chao Deng: Conceptualization, Methodology, Validation, Formal analysis, Investigation, Data curation, Writing – original draft, Writing – review & editing. **Farzad Seidi:** Supervision, Methodology, Validation, Writing – review & editing. **Qiang Yong:** Investigation, Resources, Funding acquisition. **Xiangyu Jin:** Investigation, Resources, Methodology. **Chengcheng Li:** Methodology, Validation. **Ling Zheng:** Validation, Software. **Zhenghong Yuan:** Methodology, Validation. **Huining Xiao:** Conceptualization, Supervision, Project administration, Writing – review & editing, Funding acquisition.

Declaration of Competing Interest

The authors declare that they have no known competing financial interests or personal relationships that could have appeared to influence the work reported in this paper.

Acknowledgements

The authors gratefully acknowledge the National Natural Science Foundation of China (No. 31870569) and NSERC Canada.

Compliance with ethics requirements

This article does not contain any studies with human or animal subjects.

Appendix A. Supplementary data

Supplementary data to this article can be found online at https://doi.org/10.1016/j.jare.2021.11.002.

References

[1] Zhou P, Yang X-L, Wang X-G, Hu B, Zhang L, Zhang W, et al. A pneumonia outbreak associated with a new coronavirus of probable bat origin. Nature 2020;579(7798):270–3.

[2] Ortega R, Gonzalez M, Nozari A, Canelli R. Personal protective equipment and Covid-19. N Engl J Med 2020;382(26):e105. doi: https://doi.org/10.1056/NEJMvcm2014809.

[3] Sachan D. COVID-19 pandemic has spurred materials researchers to develop antiviral masks. ACS Cent Sci 2020;6(9):1469–72.

[4] Lee J, Kim J. Material properties influencing the charge decay of electret filters and their impact on filtration performance. Polymers 2020;12(3):721.

[5] Klemeš JJ, Fan YV, Tan RR, Jiang P. Minimising the present and future plastic waste, energy and environmental footprints related to COVID-19. Renewable Sustainable Energy Rev 2020;127:109883. doi: https://doi.org/10.1016/j.rser.2020.109883.

[6] Morganti P, Morganti G. Post-COVID-19: An opportunity to produce biodegradable goods & surgical masks to save the environment. J Health Care and Research 2020;1(3):157–65.

[7] Konda A, Prakash A, Moss GA, Schmoldt M, Grant GD, Guha S. Aerosol filtration efficiency of common fabrics used in respiratory cloth masks. ACS Nano 2020;14(5):6339–47.

[8] Yim W, Cheng D, Patel SH, Kou R, Meng YS, Jokerst JV. KN95 and N95 respirators retain filtration efficiency despite a loss of dipole charge during decontamination. ACS Appl Mater Interfaces 2020;12(49):54473–80.

[9] Gope D, Gope A, Gope PC. Mask material: challenges and virucidal properties as an effective solution against coronavirus SARS-CoV-2. Open Health 2020;1(1):37–50.

[10] Seidi F, Deng C, Zhong Y, Liu Y, Huang Y, Li C, et al. Functionalized masks: Powerful materials against COVID-19 and future pandemics. Small 2021;17(42):2102453. doi: https://doi.org/10.1002/smll.v17.4210.1002/smll.202102453.

[11] Faucher S, Lundberg DJ, Liang XA, Jin X, Phillips R, Parviz D, et al. A virucidal face mask based on the reverse-flow reactor concept for thermal inactivation of SARS-CoV-2. AlChE J 2021;67(6):e17250.

[12] Kim Y-I, Kim M-W, An S, Yarin AL, Yoon SS. Reusable filters augmented with heating microfibers for antibacterial and antiviral sterilization. ACS Appl Mater Interfaces 2021;13(1):857–67.

[13] Kumar S, Karmacharya M, Joshi SR, Gulenko O, Park J, Kim G-H, et al. Photoactive antiviral face mask with self-sterilization and reusability. Nano Lett 2021;21(1):337–43.

[14] Kumar A, Sharma A, Chen Y, Jones MM, Vanyo ST, Li C, et al. Copper@ZIF-8 core-shell nanowires for reusable antimicrobial face masks. Adv Funct Mater 2021;31(10):2008054. doi: https://doi.org/10.1002/adfm.v31.1010.1002/adfm.202008054.

[15] Önal A, Özbek O, Nached S. The production of antiviral-breathing mask against SARS-CoV-2 using some herbal essential oils. J Turk Chem Soc, Sect A 2020;7(3):821–6.

[16] Rubino I, Oh E, Han S, Kaleem S, Hornig A, Lee S-H, et al. Salt coatings functionalize inert membranes into high-performing filters against infectious respiratory diseases. Sci Rep 2020;10(1). doi: https://doi.org/10.1038/s41598-020-70623-913875.

[17] Xiong S-W, Fu P-G, Zou Q, Chen L-Y, Jiang M-Y, Zhang P, et al. Heat conduction and antibacterial hexagonal boron nitride/polypropylene nanocomposite fibrous membranes for face masks with long-time wearing performance. ACS Appl Mater Interfaces 2021;13(1):196–206.

[18] Ogunsona EO, Muthuraj R, Ojogbo E, Valerio O, Mekonnen TH. Engineered nanomaterials for antimicrobial applications: A review. Appl Mater Today 2020;18:100473. doi: https://doi.org/10.1016/j.apmt.2019.100473.

[19] Huang L, Xu S, Wang Z, Xue K, Su J, Song Y, et al. Self-reporting and photothermally enhanced rapid bacterial killing on a laser-induced graphene mask. ACS Nano 2020;14(9):12045–53.

[20] Horváth E, Rossi L, Mercier C, Lehmann C, Sienkiewicz A, Forró L. Photocatalytic nanowires-based air filter: Towards reusable protective masks. Adv Funct Mater 2020;30(40):2004615. doi: https://doi.org/10.1002/adfm.v30.4010.1002/adfm.202004615.

[21] Choi M, Kim Y, Park S, Ka D, Kim T, Lee S, et al. Functionalized polyurethane-coated fabric with high breathability, durability, reusability, and protection ability. Adv Funct Mater 2021;31(24):2101511. doi: https://doi.org/10.1002/adfm.v31.2410.1002/adfm.202101511.

[22] Choi S, Jeon H, Jang M, Kim H, Shin G, Koo JM, et al. Biodegradable, efficient, and breathable multi-use face mask filter. Adv Sci 2021;8(6):2003155. doi: https://doi.org/10.1002/advs.v8.610.1002/advs.202003155.

[23] Das O, Neisiany RE, Capezza AJ, Hedenqvist MS, Försth M, Xu Q, et al. The need for fully bio-based facemasks to counter coronavirus outbreaks: A perspective. Sci Total Environ 2020;736:139611. doi: https://doi.org/10.1016/j.scitotenv.2020.139611.

[24] Belda Marin C, Fitzpatrick V, Kaplan DL, Landoulsi J, Guenin E, Egles C. Silk polymers and nanoparticles: A powerful combination for the design of versatile biomaterials. Front Chem 2020;8:604398.

[25] Chowdhury MA, Shuvho MBA, Shahid MA, Haque AKMM, Kashem MA, Lam SS, et al. Prospect of biobased antiviral face mask to limit the coronavirus outbreak. Environ Res 2021;192:110294. doi: https://doi.org/10.1016/j.envres.2020.110294.

[26] Xu Y, Zhang X, Hao X, Teng D, Zhao T, Zeng Y. Micro/nanofibrous nonwovens with high filtration performance and radiative heat dissipation property for personal protective face mask. Chem Eng J 2021;423:130175. doi: https://doi.org/10.1016/j.cej.2021.130175.

[27] Li T, Chen C, Brozena AH, Zhu JY, Xu L, Driemeier C, et al. Developing fibrillated cellulose as a sustainable technological material. Nature 2021;590(7844):47–56.

[28] Pan Y, Xiao H, Cai P, Colpitts M. Cellulose fibers modified with nano-sized antimicrobial polymer latex for pathogen deactivation. Carbohydr Polym 2016;135:94–100.

[29] Zhang D, Xiao H. Dual-functional beeswaxes on enhancing antimicrobial activity and water vapor barrier property of paper. ACS Appl Mater Interfaces 2013;5(8):3464–8.

[30] Ilkar Erdagi S, Asabuwa Ngwabebhoh F, Yildiz U. Genipin crosslinked gelatin-diosgenin-nanocellulose hydrogels for potential wound dressing and healing applications. Int J Biol Macromol 2020;149:651–63.

[31] Zhong Y, Seidi F, Li C, Wan Z, Jin Y, Song J, et al. Antimicrobial/biocompatible hydrogels dual-reinforced by cellulose as ultrastretchable and rapid self-healing wound dressing. Biomacromolecules 2021;22(4):1654–63.

[32] Pan Y, Xue Y, Snow J, Xiao H. Tailor-made antimicrobial/antiviral star polymer via ATRP of cyclodextrin and guanidine-based macromonomer. Macromol Chem Phys 2015;216(5):511–8.

[33] Deng C, Liu W, Zhang Y, Huang C, Zhao Yi, Jin X. Environmentally friendly and breathable wet-laid hydroentangled nonwovens for personal hygiene care with excellent water absorbency and flushability. R Soc Open Sci 2018;5(4):171486. doi: https://doi.org/10.1098/rsos.171486.

[34] Deng C, Gong RH, Huang C, Zhang X, Jin X-Y. Tensile strength and dispersibility of pulp/danufil wet-laid hydroentangled nonwovens. Materials (Basel) 2019;12(23):3931. doi: https://doi.org/10.3390/ma12233931.

[35] Guan Y, Xiao H, Sullivan H, Zheng A. Antimicrobial-modified sulfite pulps prepared by in situ copolymerization. Carbohydr Polym 2007;69(4):688–96.

[36] Shinoda R, Saito T, Okita Y, Isogai A. Relationship between length and degree of polymerization of TEMPO-oxidized cellulose nanofibrils. Biomacromolecules 2012;13(3):842–9.

[37] Peddinti BST, Downs SN, Yan J, Smith SD, Ghiladi RA, Mhetar V, et al. Rapid and repetitive inactivation of SARS-CoV-2 and human coronavirus on self-disinfecting anionic polymers. Adv Sci 2021;8(11):2003503. doi: https://doi.org/10.1002/advs.v8.1110.1002/advs.202003503.

[38] Zhou X, Fu Y, Chen L, Wang R, Wang X, Miao Y, et al. Diisocyanate modifiable commercial filter paper with tunable hydrophobicity, enhanced wet tensile strength and antibacterial activity. Carbohydr Polym 2020;248:116791. doi: https://doi.org/10.1016/j.carbpol.2020.116791.

[39] Ichiyama K, Yang C, Chandrasekaran L, Liu S, Rong L, Zhao Y, et al. Cooperative orthogonal macromolecular assemblies with broad spectrum antiviral activity, high selectivity, and resistance mitigation. Macromolecules 2016;49(7):2618–29.

[40] Zhang XG, Mason PW, Dubovi EJ, Xu X, Bourne N, Renshaw RW, et al. Antiviral activity of geneticin against dengue virus. Antiviral Res 2009;83(1):21–7.

[41] Bottero V, Sadagopan S, Johnson KE, Dutta S, Veettil MV, Chandran B. Kaposi's sarcoma-associated herpesvirus-positive primary effusion lymphoma tumor formation in NOD/SCID mice is inhibited by neomycin and neamine blocking angiogenin's nuclear translocation. J Virol 2013;87(21):11806–20.

[42] Szczepańska E, Bielicka-Giełdoń A, Niska K, Strankowska J, Żebrowska J, Inkielewicz-Stępniak I, et al. Synthesis of silver nanoparticles in context of their cytotoxicity, antibacterial activities, skin penetration and application in skincare products. Supramol Chem. 2020;32(3):207-21.

[43] Gralton J, McLaws M-L. Protecting healthcare workers from pandemic influenza: N95 or surgical masks? Crit Care Med 2010;38(2):657–67.